

Effects of interatomic collisions on atom laser outcoupling

Georgios M Nikolopoulos[†], P Lambropoulos^{†‡} and N P Proukakis[§]

[†] Institute of Electronic Structure & Laser, FORTH, P.O.Box 1527, Heraklion GR-71110, Crete, Greece

[‡] Department of Physics, University of Crete, P.O.Box 2208, Heraklion GR-71110, Crete, Greece

[§] Department of Physics, University of Durham, Durham DH1 3LE, United Kingdom

Abstract. We present a computational approach to the outcoupling in a simple one-dimensional atom laser model, the objective being to circumvent mathematical difficulties arising from the breakdown of the Born and Markov approximations. The approach relies on the discretization of the continuum representing the reservoir of output modes, which allows the treatment of arbitrary forms of outcoupling as well as the incorporation of non-linear terms in the Hamiltonian, associated with interatomic collisions. By considering a single-mode trapped condensate, we study the influence of elastic collisions between trapped and free atoms on the quasi steady-state population of the trap, as well as the energy distribution and the coherence of the outcoupled atoms.

PACS numbers: 03.75.-b, 03.75.Pp, 42.50.Ar, 42.50.Fx

1. INTRODUCTION

The most direct way to create an atom laser, which means an intense directional beam of coherent atoms, is based on outcoupling a pre-formed Bose-Einstein Condensate (BEC). Key constituents of such a device are the pumping mechanism replenishing the trapped condensate as atoms are outcoupled from it and the nature of the outcoupling mechanism. This has been demonstrated experimentally (for unpumped condensates) leading to the generation of pulsed [1, 2, 3] and quasi-continuous [4, 5, 6, 7, 8] atom lasers. There have been numerous theoretical treatments of the output coupling and atom lasers, and a review of the theory of atom lasers can be found in [9] and references therein. Beyond the early rate equation approaches [10, 11, 12], these can be crudely classified into mean field approaches and treatments based on master equations. Initial master equation approaches [13, 14, 15, 16, 17] were formulated within the Born-Markov approximation, whereas subsequent work [18, 19, 20, 21, 22, 23] has brought up issues pertaining to the non-Markovian character of the relevant processes and its differences from the optical laser. Moreover, not only the Markov but also the Born approximation (standard in quantum optics) is not necessarily valid. Similar issues have also arisen in recent years in the context of entirely different phenomena related to photonic crystals [24]. In particular, the behavior of an excited atom inside such a medium exhibiting a photonic band-gap (PBG) around the atomic transition frequency, has been shown to exhibit a number of features also related to the invalidation of Born and Markov approximations for the processes involved. As a consequence of the unusual density of states appearing in the coupling of the atom to the medium, a master equation which is the standard tool in laser theory and quantum optics, can not be derived in that case. This rather fundamental limitation has led to the need for alternative approaches and techniques, some of which have been proven versatile and useful [25, 26, 27, 28, 29, 30, 31].

Another common approach to the physics of atom lasers is based on mean field treatments whereby the dynamics of both trapped and outcoupled components are governed by nonlinear Schrodinger equations, with the two systems coupled by an external electromagnetic field generating the outcoupling [32, 33, 34, 35, 36, 37, 38, 39]. Nonetheless, significant insight regarding the breakdown of Born and Markov approximations can be obtained by studying the limit of a single-mode condensate, as demonstrated in [18, 19, 20, 21, 22, 23]. Although in the limit of no interactions between the trapped and the outcoupled atoms, the corresponding master equations can be solved exactly, it is still not clear, despite recent work [22], what is the effect of interactions between trapped and outcoupled atoms. In the present work, we show that one particular approach [25, 40, 41, 42], which originated in the context of atomic decay in a PBG medium, can be useful in addressing this and other related questions pertaining to the outcoupling in atom lasers. The approach we have in mind relies on the discretization of continua appearing in the equations of motion that couple the few degrees of freedom, usually referred to as “the system”, to a reservoir which, by

its nature, contains infinitely many degrees of freedom corresponding to a part of the Hamiltonian with a continuous spectrum.

In the following sections, we apply the discretization technique in the context of a one-dimensional model for an atom laser, with the limitation to one dimension due only to computational constraints. The current paper does not aim at describing the physical processes occurring in the recently-observed effectively one-dimensional systems [43, 44, 45, 46, 47, 48] which are prone to large phase fluctuations [49, 50], an issue that is dealt with in [51]. Our findings are therefore relevant to and of interest for current regimes of three-dimensional atom laser operation [1, 2, 3, 4, 5, 6, 7, 8]. We first investigate the validity of the method and study the dynamics of the trapped as well as the outcoupled atoms, in the absence of interatomic collisions between trapped and outcoupled atoms. We show that, in that context, the method allows us to treat practically exactly the problem, even for a range of parameters where it can be treated approximately. Then, we extend the treatment beyond the majority of master equation approaches that have been addressed so far in the context of atom lasers, by allowing interatomic collisions between the trapped and the untrapped (free) atoms. We discuss the assumptions under which such processes can be incorporated in our simulations and study the system dynamics under their influence.

2. OUTCOUPLING FREE OF INTERATOMIC COLLISIONS

We consider a BEC consisting of a large number of bosonic atoms cooled into a single eigenmode of a trap. The atoms are coherently coupled out of the trap by the application of external electromagnetic fields which induce an atomic transition from the internal state ($|t\rangle$) of the trapped atoms to an untrapped state $|f\rangle$ [32, 33, 38, 39, 52]. Initially, only the lowest mode of the trap is populated (condensate mode). We may further ignore the population of higher modes even at later times, if the frequency and the linewidth of the applied fields are chosen appropriately [19].

The dynamics of the system are described by a Hamiltonian of the form

$$H = H_S + H_R + V, \quad (1)$$

where H_S and H_R correspond to the trapped (system) and untrapped (reservoir) atoms, respectively, while V refers to the output coupling.

Introducing a set of bosonic operators $\{a^\dagger, a\}$ for the representation of the condensate, the corresponding Hamiltonian reads

$$H_S = \hbar\omega_0 a^\dagger a, \quad (2)$$

where ω_0 is the condensate-mode frequency. Accordingly, the part of the Hamiltonian for the free atoms is

$$H_R = \hbar \int_{-\infty}^{+\infty} dk \omega_k b_k^\dagger b_k, \quad (3)$$

where b_k^\dagger , b_k are the corresponding bosonic operators, with k being the momentum of the center-of-mass motion.

2.1. Output coupling

The condensate is coupled to the reservoir through the interaction term

$$V = \hbar \int_{-\infty}^{+\infty} dk g(k) (b_k^\dagger a + b_k a^\dagger). \quad (4)$$

In general, the form of the coupling constant $g(k)$ is determined by the type of mechanism applied to coherently couple the trapped atoms out of the trap (output coupler) [38]. For a Raman output coupling mechanism, the outcoupled state mimics the trapped condensate at short times [33, 39]. Assuming Gaussian like profile for the ground state of the harmonic trap [18, 19], the coupling constant can be approximated by

$$g(k) = \frac{\sqrt{\Gamma}}{(2\pi\sigma^2)^{1/4}} \exp(-k^2/4\sigma^2), \quad (5)$$

where Γ and σ denote the strength and the width of the coupling, respectively. Additionally, the frequency ω_k is related to the corresponding momentum by $\omega_k = \hbar k^2/2m$. It is this quadratic dependence of ω_k on k , which together with the functional dependence of $g(k)$ on k , give rise to mathematical difficulties even in this simple model. Note that, the dependence of ω_k on k is in fact identical to the analogous dispersion relation in PBG materials, which is responsible for the mathematical difficulties in that context.

For the one-dimensional problem under consideration, the density of states which are available to a free atom can be determined by the dispersion relation as follows

$$\rho(\omega) = \left| \frac{dk}{d\omega} \right| = \sqrt{\frac{m}{2\hbar\omega}} \Theta(\omega), \quad (6)$$

where m is the atomic mass and $\Theta(\omega)$ the usual step function. Taking advantage of the symmetrical shape of the coupling and the even parity of ω_k , we may reduce the k -space only to the $k > 0$ sub-space. The spectral response of the output coupling is then of the form

$$\mathcal{D}_G(\omega) = 2|g(\omega)|^2 \rho(\omega) = \frac{C}{\pi} \frac{\exp[-\omega/\alpha]}{\sqrt{\omega}} \Theta(\omega), \quad (7)$$

where the effective coupling constant C is given by

$$C = \Gamma \sqrt{\frac{\pi}{\alpha}} \quad \text{and} \quad \alpha = \frac{\hbar\sigma^2}{m}. \quad (8)$$

As σ and Γ tend to infinity, we obtain the broad-band limit of equation (7),

$$\mathcal{D}_{BB}(\omega) = \frac{C}{\pi} \frac{1}{\sqrt{\omega}} \Theta(\omega), \quad (9)$$

which is identical to the corresponding spectral response of PBG continua. Note that our model does not consider any losses due to gravity or Raman-momentum kick which could, however, have been included.

Given the Hamiltonian (1) one may proceed to derive the Heisenberg equations of motion for the operators of interest, examples of which are discussed below. At this

point, let us recall that in problems where the Born and Markov approximations are valid, as for example an excited atom decaying spontaneously in the vacuum of open space, the reservoir (continuum) variables can be eliminated. This procedure leads to a Markovian master equation governing the evolution of the system. This is what can not always be done in the present context. In the following subsection we present, for the model Hamiltonian under consideration, an approach capable of providing not only the time dependence of the number of atoms in the condensate, but also the distribution of the outcoupled atoms in frequency domain, irrespective of the strength of the coupling between the system and the reservoir. Moreover, it is applicable to more general coupling shapes and suitable for the inclusion of additional interaction terms in the Hamiltonian (see section 3) for a more realistic description of the physical situation.

2.2. Discretization of the reservoir

In order to deal with the structured reservoir, we follow the discretization approach developed in the context of PBG continua [25, 40, 41, 42]. Briefly, we substitute the reservoir for frequencies within a range around ω_0 ($\omega_{low} < \omega < \omega_{up}$), by a number (N) of discrete modes, while the rest of the atom-mode density is treated perturbatively since it is far from resonance. In general, there is no unique way of discretizing a continuum. For the sake of illustration, in the present work we apply two different discretization schemes for the Gaussian-like profile and its broad-band limit, respectively.

Specifically, for the Gaussian-like coupling we adopt a uniform discretization scheme, choosing the frequencies of the modes to be

$$\omega_j = \omega_{low} + j\delta\omega, \quad (10)$$

where the mode spacing $\delta\omega$, is determined by the upper-limit condition of the discretization, namely

$$\omega_{up} = \omega_{low} + N\delta\omega. \quad (11)$$

The corresponding coupling for the j mode, is determined by the spectral response (7) as follows

$$\mathcal{G}_j^2 = \mathcal{D}_G(\omega_j)\delta\omega. \quad (12)$$

Alternatively, for the broad-band coupling (equation 9), we may choose the integral form of equation (12), obtaining thus frequency-independent couplings for the modes, determined by

$$\mathcal{G}^2 N = \int_{\omega_{low}}^{\omega_{up}} d\omega \mathcal{D}_{BB}(\omega), \quad (13)$$

while the frequency for the j reservoir atom-mode is given by

$$\omega_j = \omega_{low} + j^2\delta\omega, \quad (14)$$

with the spacing $\delta\omega$ determined by

$$\omega_{up} = \omega_{low} + N^2\delta\omega. \quad (15)$$

Finally, note that in k -space the discretization would rely on the following equations

$$k_j = k_{low} + j\delta k, \quad \mathcal{G}_j = g(k_j)\delta k, \quad k_{up} = k_{low} + j\delta k, \quad (16)$$

from which we may obtain equations (10)-(15), using the definition of the density of atomic states (equation 6).

2.3. Heisenberg equations of motion

In the Heisenberg picture, the evolution of an arbitrary operator \mathcal{A} is governed by

$$\frac{d\mathcal{A}}{dt} = -\frac{i}{\hbar}[\mathcal{A}, H], \quad (17)$$

where H is the Hamiltonian, which for the problem at hand is determined by equations (1)-(4). Thus, for the operators of the system and the reservoir we obtain the following equations of motion

$$\frac{da}{dt} = -i\omega_0 a - 2i \int_0^\infty dk g(k) b_k dk, \quad (18)$$

$$\frac{db_k}{dt} = -i\omega_k b_k - ig(k)a, \quad (19)$$

$$\frac{d(a^\dagger a)}{dt} = -2i \int_0^\infty dk g(k)(a^\dagger b_k - b_k^\dagger a). \quad (20)$$

The solution of the above differential equations can be obtained in terms of the inverse Laplace transform. Furthermore, as has been noted in [18, 19, 20], the solution for the mean number of atoms in the condensate ($\langle a^\dagger(t)a(t) \rangle$) can be written as $\langle a^\dagger(t)a(t) \rangle = \langle a^\dagger(t) \rangle \langle a(t) \rangle$, where $\langle a(t) \rangle$ can be obtained as solution of equation (18), assuming the initial condition $\langle a(0) \rangle = \sqrt{\langle a^\dagger(0)a(0) \rangle}$, while $\langle a^\dagger(t) \rangle = \langle a(t) \rangle^*$. This assumption stems from the fact that the initial state of our model corresponds to a BEC in the atomic trap, which is a coherent state $|\beta\rangle$ of definite global phase and thus $\langle a^\dagger(0)a(0) \rangle = |\beta(0)|^2 = \langle a(0) \rangle^* \langle a(0) \rangle$. It is the bilinear form of the Hamiltonian, however, that preserves this coherence in time. What has to be noted here is that, irrespective of the initial conditions, we may obtain the evolution of $\langle a^\dagger(t)a(t) \rangle$ by combining equation (20) with the following equations of motion for $a^\dagger(t)b_k(t)$ and $b_k^\dagger(t)b_q(t)$ respectively:

$$\frac{d(a^\dagger b_k)}{dt} = -i(\omega_k - \omega_0)a^\dagger b_k - ig_k a^\dagger a + 2i \int_0^\infty dq g(q) b_q^\dagger b_k, \quad (21)$$

$$\frac{d(b_k^\dagger b_q)}{dt} = -i(\omega_q - \omega_k)b_k^\dagger b_q + ig(k)a^\dagger b_q - ig(q)ab_k^\dagger. \quad (22)$$

Discretizing the continuum over a range of frequencies ($\omega_{low} < \omega < \omega_{up}$), the integrals are converted to sums over discrete modes of frequencies $\omega_{j(m)}$, with $j(m)$ running from 1 to N , while the number of discrete modes covers only part of the reservoir. Assuming, as must be the case, that the discretized range is sufficiently large to incorporate the essential effects of the system-reservoir coupling, the remaining part of the continuum ($\omega < \omega_{low}$ and $\omega > \omega_{up}$) can be eliminated adiabatically to order of $|g(k)|^2$, in the standard fashion. Specifically, the derivative of b_k in equation

(19) for ω_k outside the discretized range, is set equal to zero, yielding the approximate solution

$$b_k(t) \approx -\frac{g(k)}{\omega_k}a(t), \quad \text{for } \omega_k < \omega_{low} \quad \text{and} \quad \omega_k > \omega_{up}. \quad (23)$$

These approximate solutions are then fed back into the equations for the operators in the discretized part of the continuum. As a consequence of this adiabatic elimination, a shift appears in the equations involving derivatives of the operators $a(a^\dagger)$ and $a^\dagger b_k(ab_k^\dagger)$. Furthermore, since the equations of motion (20) - (22) constitute a closed set of differential equations we may deal with expectation values of the operators belonging to the discretized space of the continuum, obtaining

$$\frac{d\langle a^\dagger a \rangle}{dt} = 2 \sum_{j=1}^N \mathcal{G}_j \Im\{\langle a^\dagger b_j \rangle\}, \quad (24)$$

$$\frac{d\langle a^\dagger b_j \rangle}{dt} = -i(\omega_j - \omega_0 + S)\langle a^\dagger b_j \rangle - i\mathcal{G}_j \langle a^\dagger a \rangle + i \sum_{m=1}^N \mathcal{G}_m \langle b_m^\dagger b_j \rangle, \quad (25)$$

$$\frac{d\langle b_m^\dagger b_j \rangle}{dt} = -i(\omega_j - \omega_m)\langle b_m^\dagger b_j \rangle + i\mathcal{G}_m \langle a^\dagger b_j \rangle - i\mathcal{G}_j \langle a^\dagger b_m \rangle^*, \quad (26)$$

where for simplicity of notation, ω_r , \mathcal{G}_r and b_r stand for ω_{k_r} , \mathcal{G}_{k_r} and b_{k_r} respectively, with $r \in \{j, m\}$, while $\Im\{\cdot\}$ denotes the imaginary part of the expression inside the curly braces. The shift term is given by

$$S = \int_0^{\omega_{low}} d\omega \frac{\mathcal{D}(\omega)}{\omega} + \int_{\omega_{up}}^{\infty} d\omega \frac{\mathcal{D}(\omega)}{\omega}, \quad (27)$$

where $\mathcal{D}(\omega) = \mathcal{D}_{G(BB)}(\omega)$ and the lower bound of the first integral has been set to zero as dictated by the step function in the spectral responses of the reservoir. Furthermore, in the above set of equations we have used the fact that for each pair of arbitrary operators \mathcal{A} and \mathcal{B} we have $(\mathcal{A}\mathcal{B})^\dagger = \mathcal{B}^\dagger \mathcal{A}^\dagger$ and thus $\langle \mathcal{A}\mathcal{B} \rangle^* = \langle \mathcal{B}^\dagger \mathcal{A}^\dagger \rangle$. The same equality allows us to deal with half of the matrix elements $\langle b_m^\dagger b_j \rangle$, those which involve $m \leq j$ since the elements involving $j < m$ can be obtained by $\langle b_m^\dagger b_j \rangle = \langle b_j^\dagger b_m \rangle^*$.

In the following sections, we present some selected results for the above discretized set of differential equations. Specifically, for various values of the parameters and for both Gaussian and broad-band couplings, we investigate the time dependence of the number of atoms in the condensate and the energy distribution of the outcoupled atoms $\langle b_k^\dagger b_k \rangle$.

At this point, some general remarks need to be made concerning the expected accuracy of the discretization approach. Two main parameters enter the system of equations, namely the number of modes N and the upper(lower) limit of the discretized part of the continuum. The number of modes will determine the maximum time for which the numerical solution of the discretized system can be considered accurate. This is already known from the experience gained in PBG media. If one wants to obtain a correct solution for longer times (and this is the case for larger values of coupling, when a steady state is reached more slowly), one has to increase the number of modes and the number of differential equations, which scales roughly as N^2 .

On the other hand, the parameters ω_{up} and ω_{low} must be chosen so that $\omega_{up} - \omega_{low}$ is large enough to include all modes with significant role (for sure it must be chosen such that $\omega_{low} < \omega_0 < \omega_{up}$) but also such that the spacing $\delta\omega$ will produce a smooth enough energy spectrum. As a general remark pertaining to the results discussed below, we note that the convergence of our calculations has been checked in terms of the number of discrete modes as well as the range of discretization. As is depicted in figure 1, in order to reproduce the results obtained by means of the Laplace transform in the context of Gaussian couplings (solid line) [20], we find that we need at least 500 discrete modes (dot-dashed line) and a value of 3 for ω_{up} in units of $C^{2/3}$. As far as the short-time and the long-time behavior are concerned (in which we are mainly interested), we may obtain the dynamics of the system even for 50 or 60 modes and $\omega_{up} = 3$ (dotted line), avoiding thus time-consuming numerical calculations which are expected to add quantitative and not qualitative corrections to our results. For the broad-band coupling (inset) the situation is slightly different, in the sense that the solution obtained with 50 discrete modes (dotted line) is almost indistinguishable from the exact solution (solid line). Nevertheless, as a consequence of the discretized continuum, it exhibits revivals for longer times, which are expected to appear for later and later times as we increase the number of discrete modes.

To facilitate comparison with the results of Moy et al. [19, 20], throughout this paper we consider $m = 5 \times 10^{-26} kg$, $\omega_0 = 2\pi \times 123 sec^{-1}$ and $\sigma = 10^6 m^{-1}$. Since, however, the time scale on which the main dynamics take place is expected to be strongly dependent on the coupling parameters, from now on we present the dynamics of the system as a function of the dimensionless time $C^{2/3}t$.

2.4. Dynamics

In figure 2(a), we present the time evolution of the normalized mean number of atoms (population) in the condensate mode for Gaussian coupling and various values of Γ . As was expected, for weak couplings in relation to ω_0 , the trap mode exhibits a Markovian behavior in the sense that its population decays exponentially to zero (long-dashed line). As we increase the coupling strength, however, the trap population begins exhibiting non-Markovian features. Specifically, after a transient regime where part of the initial population is lost, the system undergoes Rabi-like oscillations. These oscillations can be interpreted as a beating of the system between two different paths associated with the two characteristic frequencies of the problem, namely the trap-mode frequency ω_0 and the singularity $\omega = 0$, where the spectral response is peaked. The crucial role of these two characteristic points in the system dynamics, is also reflected in the energy distribution of the outcoupled atoms [figures 2(b)-(d)] which, for relatively large couplings, exhibits peaks at $\omega = \omega_0$ and $\omega \approx 0$, respectively. In the weak-coupling regime, the peak at ω_0 is prominent. As we enter the strong coupling regime, however, a larger part of the continuum is involved and thus, on the one hand the distribution becomes broader while on the other, the Gaussian coupling tends to couple the cavity

mode not only to modes with frequencies in the vicinity of ω_0 , but also to low-energy modes ($\omega \approx 0$). Furthermore, the central frequency of the distribution is shifted towards higher frequencies. This behavior is analogous to the shift in the levels of a two-level atom coupled to a photonic continuum and in the context of atom lasers has also been noted by Jeffers and co-workers [53].

From the physical point of view, the oscillations in the trap population stem from the outcoupled atoms which are fed back into the trapped state, reexciting thus the condensate mode. Due to this back action of the reservoir, the system finally reaches a steady state where the condensate mode is partly excited. With increasing coupling strength, the oscillations become more pronounced and faster, while the population trapping in the cavity increases. As is evident in figure 3, the non-zero steady-state trap population is also associated with strong coherence between the atoms in the trap and the outcoupled atoms (upper graphs), as well as between the free atoms (lower graphs). Although for weak couplings the coherence is negligible and is restricted to the vicinity of the trap-mode frequency, it increases rapidly for increasing values of the coupling strength, while simultaneously it spreads out to a larger number of modes. This behavior clearly indicates the departure of the system from the Markovian dynamics. In figure 3 we note that the index of the discrete mode corresponding to the trap-mode frequency ω_0 , is given by

$$j_0 = \left[\frac{(\omega_0 - \omega_{low})N}{\omega_{up} - \omega_{low}} \right], \quad (28)$$

where $[x]$ denotes the integer part of x .

For the broad-band coupling (figure 4), the dynamics are basically the same. The broad-band nature of the coupling, however, allows a significant interaction with more continuum states. Thus, the system reaches steady state much faster, while the oscillations in the cavity population are not so pronounced. Moreover, the energy distribution of the outcoupled atoms is much broader than in the Gaussian coupling.

3. INTERATOMIC COLLISIONS

Up to now we have not considered any collisional interactions between trapped and free atoms in our model. As a result, we had to deal with a Hamiltonian bilinear in the field operators and thus with a closed set of linear differential equations for the operators of interest. In real condensates, however, interatomic collisions take place and affect, in most cases, the dynamics of the system significantly. Specifically, considering a small rate of output from the trap, the output atomic beam is dilute and thus, we may neglect collisional interactions between free atoms. We may further ignore inelastic collisions between untrapped and trapped atoms, since the corresponding mean free path is much larger than the dimensions of a typical atomic condensate in the trap.

In our subsequent discussion, we focus on the elastic collisions of the untrapped atoms with those in the trap. Considering low-energy s -wave scattering of length

a_s between trapped and free atoms, we may adopt a standard hard-core interatomic potential which for a three-dimensional model in position representation is

$$\tilde{U}_{tf}(\mathbf{r} - \mathbf{r}') = U_{tf}^{(3D)}\delta(\mathbf{r} - \mathbf{r}'), \quad (29)$$

where $U_{tf}^{(3D)} = 4\pi\hbar^2 a_s/m$. For the model at hand, however, we have to derive an one-dimensional, approximate form of equation (29), capable of providing us with an estimate of the importance of interactions in our model. In the case of tight transverse confinement, the scattering strength can be well approximated by integrating out the transverse directions leading to [54]

$$\tilde{U}_{tf}(x - x') \approx \frac{U_{tf}^{(3D)}}{2\pi a_{ho}^2} \delta(x - x') = 2\hbar a_s \omega_{\perp} \delta(x - x'), \quad (30)$$

where ω_{\perp} the transverse confining frequency and $a_{ho} = \sqrt{\hbar/m\omega_{\perp}}$ the corresponding harmonic-oscillator length. In this paper we are not concerned with the limit of reduced dimensionality [43] and we have only limited ourselves to one-dimensional simulations for computational ease. The corresponding part of the Hamiltonian then takes the form

$$V_{tf} = \hbar \int_{-\infty}^{+\infty} dk \int_{-\infty}^{+\infty} dq \kappa(k, q) b_k^{\dagger} b_q a^{\dagger} a, \quad (31)$$

where, for a Gaussian ground state of the trap, the coupling constant $\kappa(k, q)$ reads,

$$\kappa(k, q) = \mathcal{N} a_s \omega_{\perp} \exp\left[-\frac{(k - q)^2}{8\sigma^2}\right], \quad (32)$$

with \mathcal{N} being the number of trapped atoms. Note that the coupling constant is symmetric with respect k and q and thus V_{tf} is Hermitian.

In analogy to the output coupling, the spectral response for interparticle interactions can be defined as

$$\mathcal{M}_G(\omega, \omega') = 4|\kappa(\omega, \omega')|^2 \rho(\omega) \rho(\omega') = C_M \frac{\exp[-(\sqrt{\omega} - \sqrt{\omega'})^2/2\alpha]}{\sqrt{\omega\omega'}} \Theta(\omega) \Theta(\omega'), \quad (33)$$

where the effective interatomic coupling C_M is

$$C_M = \frac{2\mathcal{N}^2 a_s^2 \omega_{\perp}^2 m}{\hbar}. \quad (34)$$

As σ and Γ tend to infinity, we obtain the broad-band limit of equation (33):

$$\mathcal{M}_{BB}(\omega, \omega') = C_M \frac{1}{\sqrt{\omega\omega'}} \Theta(\omega) \Theta(\omega'). \quad (35)$$

For $a_s \approx 1nm$ and $m \approx 5 \times 10^{-26}kg$, we have $C_M \approx 10^{-9}(\mathcal{N}\omega_{\perp})^2 sec$. A reasonable estimate of realistic interatomic coupling strengths in our model, can be obtained by noting that, for $\mathcal{N} \approx 10^3$ atoms and $\omega_{\perp} \approx 2\pi \times 1000sec^{-1}$, a typical value for C_M is $C_M \approx 10^4 sec^{-1}$, or else $C_M \approx 10C^{2/3}$.

3.1. Heisenberg equations of motion

Having now included interatomic collisions in our model, the Hamiltonian is not bilinear and the equations of motion for the operators of interest are no longer linear. Specifically, using equation (17) we obtain the following set of differential equations

$$\frac{d\langle a^\dagger a \rangle}{dt} = -2i \int_0^\infty dk g(k) (a^\dagger b_k - b_k^\dagger a), \quad (36)$$

$$\begin{aligned} \frac{d\langle a^\dagger b_k \rangle}{dt} &= -i(\omega_k - \omega_0) a^\dagger b_k - i g_k a^\dagger a + 2i \int_0^\infty dq g(q) b_q^\dagger b_k - 2i \int_0^\infty dq \kappa(k, q) a^\dagger b_q a^\dagger a \\ &\quad + 4i \int_0^\infty dq \int_0^\infty dq' \kappa(q, q') b_q^\dagger b_{q'} a^\dagger b_k, \end{aligned} \quad (37)$$

$$\begin{aligned} \frac{d\langle b_k^\dagger b_q \rangle}{dt} &= -i(\omega_q - \omega_k) b_k^\dagger b_q + i g(k) a^\dagger b_q - i g(q) a b_k^\dagger - 2i \int_0^\infty dk' \kappa(q, k') a^\dagger a b_k^\dagger b_{k'} \\ &\quad + 2i \int_0^\infty dk' \kappa(k', k) a^\dagger a b_{k'}^\dagger b_q, \end{aligned} \quad (38)$$

which can not be solved by means of the Laplace transform.

In order to proceed to the solution of the above equations in the context of the discretization approach, we have to incorporate appropriately the interatomic collisions in the discretization schemes developed earlier in section 2. To this end, we assume that the interatomic coupling spans the same discretized space with the output coupling and thus does not affect the far off-resonant b_k operators. This assumption, on the one hand, allows us to adiabatically eliminate the same b_k as before, while on the other to use the same discrete modes for both the output and the interatomic couplings. Note that in the case of trap-trap interatomic interactions, an adiabatic elimination procedure of the high-lying modes has been shown to lead to the renormalization of the (bare) interatomic potential to an effective one given by the usual pseudopotential of equation (29) [55, 56]. We believe it is therefore consistent here to adiabatically eliminate high-lying modes (of the output spectrum) to obtain s-wave scattering between trapped and outcoupled atoms. Consideration of low-energy s-wave scattering for interatomic collisions implies that our discretization should be applied under the constrain $k_{up} a_s \ll 1$. To confirm this, note that for the parameters used in the paper, $k_{up} \approx 10^6 m^{-1}$ and $a_s \approx 10^{-9} m$ and thus $k_{up} a_s \approx 10^{-3} \ll 1$.

Extending equations (12) and (13) to the two-dimensional (k_m, k_j) space we introduce the following coupling constants which involve pairs of modes:

$$\mathcal{G}_{mj}^2 = \mathcal{M}_G(\omega_m, \omega_j) \delta\omega \delta\omega. \quad (39)$$

$$\mathcal{G}_{int}^2 N^2 = \int_{\omega_{low}}^{\omega_{up}} d\omega' \int_{\omega_{low}}^{\omega_{up}} d\omega \mathcal{M}_{BB}(\omega, \omega'), \quad (40)$$

and correspond to the uniform and the non-uniform discretization scheme, respectively. We thus obtain the following set of equations of motion for the expectation values of the operators involving the discrete part of the continuum

$$\frac{d\langle a^\dagger a \rangle}{dt} = 2 \sum_{j=1}^N \mathcal{G}_j \mathfrak{F} \{ \langle a^\dagger b_j \rangle \}, \quad (41)$$

$$\begin{aligned} \frac{d\langle a^\dagger b_j \rangle}{dt} &= -i(\omega_j - \omega_0 + S)\langle a^\dagger b_j \rangle - i\mathcal{G}_j \langle a^\dagger a \rangle + i \sum_{m=1}^N \mathcal{G}_m \langle b_m^\dagger b_j \rangle - i \sum_{m=1}^N \mathcal{G}_{jm} \langle a^\dagger b_m a^\dagger a \rangle \\ &\quad + i \sum_{l,m=1}^N \mathcal{G}_{lm} \langle b_l^\dagger b_m a^\dagger b_j \rangle, \end{aligned} \quad (42)$$

$$\begin{aligned} \frac{d\langle b_m^\dagger b_j \rangle}{dt} &= -i(\omega_j - \omega_m)\langle b_m^\dagger b_j \rangle + i\mathcal{G}_m \langle a^\dagger b_j \rangle - i\mathcal{G}_j \langle a^\dagger b_m \rangle^* - i \sum_{l=1}^N \mathcal{G}_{jl} \langle a^\dagger a b_m^\dagger b_l \rangle \\ &\quad + i \sum_{l=1}^N \mathcal{G}_{lm} \langle a^\dagger a b_l^\dagger b_j \rangle, \end{aligned} \quad (43)$$

which is not closed. The structure of these equations is a typical case of equations of motion emerging from Hamiltonians involving terms of order higher than bilinear. The main feature is the presence in the right hand side of operators of order higher than the one whose derivative is considered. Consideration of differential equations for those higher order correlation functions leads to the appearance of terms of even higher order and so on. The system of equations, in other words, does not close and there are no general exact remedies.

One way to obtain an approximate solution is to decorrelate the higher order correlation functions into products of lower ones. Again, there usually is more than one way of doing so, the only guide being the demand for a closed system of equations. Perhaps the most straightforward decorrelation suggesting itself in the system of equations (41)-(43) is to decorrelate products of four operators in a way such that the decorrelated parts involve equal number of raising and lowering operators i.e., $\langle a^\dagger b_m a^\dagger a \rangle \approx \langle a^\dagger a \rangle \langle a^\dagger b_m \rangle$, $\langle b_l^\dagger b_m a^\dagger b_j \rangle \approx \langle b_l^\dagger b_m \rangle \langle a^\dagger b_j \rangle$ and $\langle a^\dagger a b_m^\dagger b_l \rangle \approx \langle a^\dagger a \rangle \langle b_m^\dagger b_l \rangle$. We thus have the set of equations A:

$$\frac{d\langle a^\dagger a \rangle}{dt} = 2 \sum_{j=1}^N \mathcal{G}_j \Im \{ \langle a^\dagger b_j \rangle \}, \quad (44)$$

$$\begin{aligned} \frac{d\langle a^\dagger b_j \rangle}{dt} &= -i(\omega_j - \omega_0 + S)\langle a^\dagger b_j \rangle - i\mathcal{G}_j \langle a^\dagger a \rangle + i \sum_{m=1}^N \mathcal{G}_m \langle b_m^\dagger b_j \rangle - i \langle a^\dagger a \rangle \sum_{m=1}^N \mathcal{G}_{jm} \langle a^\dagger b_m \rangle \\ &\quad + i \langle a^\dagger b_j \rangle \sum_{l,m=1}^N \mathcal{G}_{lm} \langle b_l^\dagger b_m \rangle, \end{aligned} \quad (45)$$

$$\begin{aligned} \frac{d\langle b_m^\dagger b_j \rangle}{dt} &= -i(\omega_j - \omega_m)\langle b_m^\dagger b_j \rangle + i\mathcal{G}_m \langle a^\dagger b_j \rangle - i\mathcal{G}_j \langle a^\dagger b_m \rangle^* - i \langle a^\dagger a \rangle \sum_{l=1}^N \mathcal{G}_{jl} \langle b_m^\dagger b_l \rangle \\ &\quad + i \langle a^\dagger a \rangle \sum_{l=1}^N \mathcal{G}_{lm} \langle b_l^\dagger b_j \rangle. \end{aligned} \quad (46)$$

Applying the commutation relation $[b_m, b_n^\dagger] = \delta_{mn}$ in equation (43) and decorrelating in the same fashion the resulting equation, we have an alternative form for equation (46):

$$\begin{aligned} \frac{d\langle b_m^\dagger b_j \rangle}{dt} &= -i(\omega_j - \omega_m)\langle b_m^\dagger b_j \rangle + i\mathcal{G}_m \langle a^\dagger b_j \rangle - i\mathcal{G}_j \langle a^\dagger b_m \rangle^* - i \langle a^\dagger b_m \rangle^* \sum_{l=1}^N \mathcal{G}_{jl} \langle a^\dagger b_l \rangle \\ &\quad + i \langle a^\dagger b_j \rangle \sum_{l=1}^N \mathcal{G}_{lm} \langle a^\dagger b_l \rangle^*, \end{aligned} \quad (47)$$

which combined with equations (44) and (45) constitute another closed set of differential equations (set B).

3.2. Dynamics

In the absence of interatomic collisions the effective coupling constant C is the one that determines the time scale of the initial transient regime i.e., the speed at which the trap-mode loses population for short time. In the present case, however, interatomic collisions are expected to be the dominant processes for short times, determining thus the corresponding time scale. Both sets of equations (A and B) predict the same dynamics for the system. In figure 5, we plot the solutions for the population in the trap as a function of the dimensionless time $C^{2/3}t$ obtained through the set of equations B. Clearly, the rate at which the trap loses population decreases with increasing values of C_M while the trap-mode excitation undergoes oscillations which reflect the interference between the two possible decay routes for the system, corresponding to ω_0 and $\omega = 0$, respectively.

The functional dependence of $\mathcal{M}(\omega, \omega')$ on ω and ω' , respectively, reveals the main role of interatomic collisions, namely the decoherence. We know already (section 2) that the coherence between the atoms is associated with the non-Markovian behavior of the system and the partial depletion of the excitation of the initially highly populated condensate-mode. Under the influence of interatomic collisions, however, the coherence between the outcoupled atoms is reduced and is restricted to the vicinity of the trap-mode frequency (see lower graphs in figure 6), leading thus to a significant decay of the initially trapped atomic population, as well as a narrow distribution of the energies of the outcoupled atoms around ω_0 [figures 6(a)-(d)]. This is in analogy to the behavior of the system in the absence of interatomic collisions and for weak output couplings (see lower graphs in figure 3, for $\Gamma = 10^4 - 10^5 \text{sec}^{-2}$). It could thus be argued that the dynamics of the system are governed by a set of equations of motion of the form

$$\frac{d\langle a^\dagger a \rangle}{dt} = 2 \sum_{j=1}^N \mathcal{G}_j \Im\{\langle a^\dagger b_j \rangle\}, \quad (48)$$

$$\begin{aligned} \frac{d\langle a^\dagger b_j \rangle}{dt} = & -i(\omega_j - \omega_0 + S)\langle a^\dagger b_j \rangle - i\mathcal{G}_j \langle a^\dagger a \rangle + i\mathcal{G}_j \langle b_j^\dagger b_j \rangle - i\langle a^\dagger a \rangle \sum_{m=1}^N \mathcal{G}_{jm} \langle a^\dagger b_m \rangle \\ & + i\langle a^\dagger b_j \rangle \sum_{m=1}^N \mathcal{G}_{mm} \langle b_m^\dagger b_m \rangle, \end{aligned} \quad (49)$$

$$\frac{d\langle b_m^\dagger b_m \rangle}{dt} = -2\mathcal{G}_m \Im\{\langle a^\dagger b_m \rangle\} - 2 \sum_{l=1}^N \mathcal{G}_{lm} \Im\{\langle a^\dagger b_m \rangle \langle a^\dagger b_l \rangle^*\}, \quad (50)$$

where no coherences between the outcoupled atoms are involved. As depicted in the inset of figure 5, this argument is indeed true for short times and relatively large interatomic couplings, where interatomic collisions dominate over the output coupling. As was expected, however, the above set of equations fail to describe the decoherence in our model for larger times. Alternative decorrelation schemes and their predictions about

the system dynamics are discussed in the Appendix.

4. SUMMARY

We have presented an alternative approach to a simple model for atom laser outcoupling which is capable of circumventing certain mathematical difficulties arising from the breakdown of the Born and Markov approximations, inherent in essentially any model of the process. The approach is computational, relying on the discretization of the continuum representing the reservoir of the outcoupled atoms and has been recently developed in the context of PBG continua. To provide a calibration of the possibilities offered by the method, we presented representative results, some of which serve as a basis for comparison with previous work relying on different methods, while others demonstrate how this approach can go beyond the above mentioned limitations.

In particular, we have studied the dynamics of a single-mode trapped condensate which, in order to form an atom laser, is outcoupled by both Gaussian and broad-band couplings. In the model considered here, there is no mechanism to remove the outcoupled atoms, and the ensuing coupling between trapped and outcoupled atoms provides (in certain limits) a striking manifestation of the non-markovian nature of the outcoupling. For example, considering initially a situation in which condensate and outcoupled atoms do not interact, we have shown that, after an initial transient regime where part of the trapped atomic population is lost, the system reaches a steady state for which the population inside the trap has not been totally depleted. This non-markovian nature is most pronounced when outcoupling at a rate larger than (or comparable to) the trap frequency, and is also evident in the coherences between trapped-outcoupled, or outcoupled-outcoupled atoms, which additionally experience a peak around $\omega \approx 0$.

These coherences thus play a significant role in the time evolution of the system. Perhaps more significant is the effect that the addition of interactions between condensate and outcoupled atoms has on the outcoupled spectrum. It has been previously argued that interatomic interactions could potentially destroy this ‘bound mode’ of atoms within the trap. In this work we have explicitly considered the effect of interactions between trapped and outcoupled atoms and have shown directly that realistic interaction strengths will largely destroy this ‘bound mode’. Interatomic interactions also have a drastic effects on the coherences between trapped and outcoupled atoms. We have thus shown that our computational approach is capable of exploring the entire domain of outcoupling from non-markovian to markovian, and can additionally include atom-atom interactions.

It should be stressed that this paper only describes the mechanism of outcoupling, and does not deal with the full complexity of an actual atom laser. In particular, we have assumed that we begin with a single-mode condensate, without any thermal excitations being present. Thus, strictly-speaking, our treatment is restricted to the zero temperature limit. Consideration of excitations into our model will lead firstly, to a decrease in the amount of coherence present in the trapped system. This will subsequently limit the coherence transferred to the outcoupled beam (atom laser), with the extent of the decrease from the purely condensed case, depending on the particular

choice of the outcoupling, since some thermal component will be inevitably outcoupled. This point has been discussed in [34, 35], whereas a three-dimensional treatment for Raman pulsed atom lasers has been recently performed [57].

The model considered here, does not account for a mechanism of removal of the outcoupled atoms. Such a mechanism arises naturally from the effect of gravity, and can also be controlled by the amount of momentum imparted to the outcoupled atoms via Raman outcoupling. When the outcoupled atoms are removed from the system, the only way to reach the desired steady state is by continuously pumping the trapped condensate. Both of these features are essential in the steady-state operation of an atom laser, and can be included without particular difficulty in an extended version of our presented model. However, it bears repeating that the main aim of this paper was not to describe the full atom laser operation, but rather to introduce an alternative method for describing the process of outcoupling. A model dealing with a cw atom laser in a one-dimensional waveguide by means of a Langevin equation, where issues such as the laser linewidth can be addressed has been discussed by one of us elsewhere [51].

One of the important features of the method employed in this paper is the versatility in handling any form of functional dependence of the outcoupling on the atomic momentum. Furthermore, it is amenable to the study of further properties of the system such as higher order correlation functions, albeit, as it appears for the moment, within the limits of some form of decorrelation. Although the various decorrelation approximations we had to resort to have given more or less qualitatively compatible results, still the task of narrowing the possible choices needs to be addressed. One avenue in that direction would be the examination of higher order of correlation functions, with the ultimate limitation being the size of the computation, as the model becomes more complex. Computational possibilities, on the other hand, are not frozen but increase constantly. Clearly, analytically solvable models are indispensable in the insight they offer, but computational approaches are often necessary in examining details of the dynamics of a complex system.

Appendix A. Alternative decorrelation schemes

In general there is no unique way of decorrelating a system of coupled Heisenberg equations of motion. In the main body of the paper, we have already presented two different decorrelation schemes. We discuss two more in this appendix. Applying the commutation relation $[b_m^\dagger, b_j] = \delta_{mj}$ in equation (42), we obtain

$$\begin{aligned} \frac{d\langle a^\dagger b_j \rangle}{dt} &= -i(\omega_j - \omega_0 + S)\langle a^\dagger b_j \rangle - i\mathcal{G}_j\langle a^\dagger a \rangle + i\sum_{m=1}^N \mathcal{G}_m\langle b_m^\dagger b_j \rangle - i\sum_{m=1}^N \mathcal{G}_{jm}\langle a^\dagger b_m a^\dagger a \rangle \\ &\quad + i\sum_{l,m=1}^N \mathcal{G}_{lm}\langle b_m b_l^\dagger a^\dagger b_j \rangle - i\langle a^\dagger b_j \rangle \sum_{l=1}^N \mathcal{G}_{ll} \end{aligned} \quad (\text{A.1})$$

which can be decorrelated as follows

$$\begin{aligned} \frac{d\langle a^\dagger b_j \rangle}{dt} &= -i(\omega_j - \omega_0 + S)\langle a^\dagger b_j \rangle - i\mathcal{G}_j\langle a^\dagger a \rangle + i\sum_{m=1}^N \mathcal{G}_m\langle b_m^\dagger b_j \rangle - i\langle a^\dagger a \rangle \sum_{m=1}^N \mathcal{G}_{jm}\langle a^\dagger b_m \rangle \\ &\quad + i\sum_{l,m=1}^N \mathcal{G}_{lm}\langle a^\dagger b_m \rangle \langle b_l^\dagger b_j \rangle - i\langle a^\dagger b_j \rangle \sum_{l=1}^N \mathcal{G}_{ll}. \end{aligned} \quad (\text{A.2})$$

This equation of motion can replace equation (45) in the sets of equations we presented in the previous sections. The resulting sets of equations, however, predict substantially different behavior for the system than the one discussed up to now. Specifically, we have found that the number of the outcoupled atoms decreases significantly for large values of C_M in relation to $C^{2/3}$. Thus, the atomic population of the trap tends to remain trapped forever ($\langle a^\dagger(t)a(t) \rangle \approx 1$). Actually, this behavior stems from the last factor in equation (A.2), which leads to a non-dissipative Rabi-like oscillation of the cavity population close to unity i.e., $\langle a^\dagger(t)a(t) \rangle \approx 1 - \exp(-i\sum_l \mathcal{G}_{ll}t)$. We may overcome this problem by decorrelating the last term in equation (42) as $\langle b_l^\dagger b_m a^\dagger b_j \rangle \approx \langle a^\dagger b_m \rangle \langle b_l^\dagger b_j \rangle$ obtaining thus equation (A.2) without the term involving \mathcal{G}_{ll} .

Using the corresponding commutation relation for the cavity-mode operators i.e., $[a, a^\dagger] = 1$, we obtain from equation (43)

$$\begin{aligned} \frac{d\langle b_m^\dagger b_j \rangle}{dt} &= -i(\omega_j - \omega_m)\langle b_m^\dagger b_j \rangle + i\mathcal{G}_m\langle a^\dagger b_j \rangle - i\mathcal{G}_j\langle a^\dagger b_m \rangle^* + i\sum_{l=1}^N \mathcal{G}_{jl}\langle b_m^\dagger b_l \rangle - i\sum_{l=1}^N \mathcal{G}_{lm}\langle b_l^\dagger b_j \rangle \\ &\quad - i\sum_{l=1}^N \mathcal{G}_{jl}\langle a a^\dagger b_m^\dagger b_l \rangle + i\sum_{l=1}^N \mathcal{G}_{lm}\langle a a^\dagger b_l^\dagger b_j \rangle, \end{aligned} \quad (\text{A.3})$$

which after decorrelation reads

$$\begin{aligned} \frac{d\langle b_m^\dagger b_j \rangle}{dt} &= -i(\omega_j - \omega_m)\langle b_m^\dagger b_j \rangle + i\mathcal{G}_m\langle a^\dagger b_j \rangle - i\mathcal{G}_j\langle a^\dagger b_m \rangle^* + i\sum_{l=1}^N \mathcal{G}_{jl}\langle b_m^\dagger b_l \rangle - i\sum_{l=1}^N \mathcal{G}_{lm}\langle b_l^\dagger b_j \rangle \\ &\quad - i\sum_{l=1}^N \mathcal{G}_{jl}\langle a^\dagger b_m \rangle^* \langle a^\dagger b_l \rangle + i\sum_{l=1}^N \mathcal{G}_{lm}\langle a^\dagger b_l \rangle^* \langle a^\dagger b_j \rangle. \end{aligned} \quad (\text{A.4})$$

Although this equation of motion, accompanied by equations (44), (45), predict mainly the same short-time dynamics that we have discussed in section 3, it overestimates the quasi-steady state of the trap-mode as well as the oscillations in the cavity excitation.

In other words, equation (A.4) seems to overestimate the coherences in our system, due to the appearance of terms like $\sum_{l=1}^N \mathcal{G}_{lm} \langle b_l^\dagger b_j \rangle$ in its right-hand side.

Acknowledgments

NPP would like to acknowledge financial support from the U.K. EPSRC.

References

- [1] Mewes M O, Andrews M R, Kurn D M, Durfee D S, Townsend C G, and Ketterle W *Phys. Rev. Lett.* **78** 582 (1997); Andrews M R, Townsend C G, Miesner H J, Durfee D S, Kurn D M, and Ketterle W *Science* **275** 637 (1997)
- [2] Anderson, B P and Kasevich M A *Science* **282** (1998)
- [3] Martin J L, McKenzie C R, Thomas N R, Sharpe J C, Warrington D M, Manson P J, Sandle W J and Wilson A C *J. Phys. B* **32** 3065 (1999)
- [4] Bloch I, Hänsch T W and Esslinger T *Phys. Rev. Lett.* **82** 3008 (1999)
- [5] Bloch I, Hänsch T W, and Esslinger T *Nature* **403** 166 (2000)
- [6] Hagley E W, Deng L, Kozuma M, Wen J, Helmerson K, Rolston S L, and Phillips W D *Science* **283** 1706 (1999)
- [7] Minardi F, Fort C and Maddaloni P *Proceedings of the 27th School of Quantum Electronics: Bose-Einstein Condensation and Atom Lasers*, Martellucci, S., Chester, A. N., Aspect, and Inguscio M (edt.) (Kluwer Academic, 2000).
- [8] Le Coq Y, Thywissen J H, Rangwala S A, Gerbier F, Richard S, Delannoy G, Bouyer P and Aspect A *Phys. Rev. Lett.* **87** 170403 (2001)
- [9] Ballagh R and Savage C M, in *Bose-Einstein Condensation: from atomic physics to quantum fluids, Proceedings of the 13th Physics Summer School*, edited by C. Savage and M. Das (World Scientific, Singapore, 2000).
- [10] Olshanii M, Castin Y and Dalibard J, in *Proceedings of the 12th International Conference on Laser Spectroscopy*, edited by M. Inguscio, M. Allegrini and A. Sasso (World Scientific, 1995).
- [11] Spreuw R J C, Pfau T, Janicke U and Wilkens M *Europhys. Lett.* **32** 469 (1995)
- [12] Moy G M, Hope J J and Savage C M *Phys. Rev. A* **55** 3631 (1997)
- [13] Holland M, Burnett K, Gardiner C, Cirac J I and Zoller P *Phys. Rev. A* **54** R1757 (1996)
- [14] Wiseman H, Martins A and Walls D J *Opt. B: Quant. Semiclass. Opt.* **8**, 737 (1996)
- [15] Guzman A, Moore M and Meystre P *Phys. Rev. A* **53** 977 (1996)
- [16] Zobay O and Meystre P *Phys. Rev. A* **57** 4710 (1998)
- [17] Wiseman H M, Burnett K and Collett M J *J. Phys. B* **32** 3669 (1999)
- [18] Hope J J *Phys. Rev. A* **55** R2531 (1997)
- [19] Moy G M and Savage C M *Phys. Rev. A* **56** R1087 (1997)
- [20] Moy G M, Hope J J and Savage C M *Phys. Rev. A* **59** 667 (1999)
- [21] Hope J J, Moy G M, Collett M J and Savage C M *Phys. Rev. A* **61** 023603 (2000)
- [22] Jack M W, Naraschewski M, Collett M J and Walls D F *Phys. Rev. A* **59** 2962 (1999)
- [23] Breuer H P, Faller D, Kappler B and Petruccione F *Phys. Rev. A* **60** 3188 (1999)
- [24] Lambropoulos P, Nikolopoulos G M, Nielsen T R and Bay S *Rep. Prog. Phys.* **63** 455 (2000)
- [25] Nikolopoulos G M, Bay S and Lambropoulos P *Phys. Rev. A* **60** 5079 (1999).
- [26] Strunz W T, Diosi L and Gisin N *Phys. Rev. Lett* **82** 1801 (1999).
- [27] Diosi L, Gisin N and Strunz W T *Phys. Rev. A* **58** 1699 (1998)
- [28] Garraway B M *Phys. Rev. A* **55** 2290 (1997)
- [29] Jack M W and Hope J J *Phys. Rev. A* **63** 043803 (2001)
- [30] Breuer H P, Kappler B and Petruccione F *Phys. Rev. A* **59** 1633 (1999)
- [31] Gambetta J and Wiseman H M *Phys. Rev. A* **66** 012108 (2002); *ibid.* 052105 (2002)

- [32] Ballagh R J, Burnett K and Scott T F *Phys. Rev. Lett* **78** 1607 (1997)
- [33] Jackson B, McCann J F and Adams C S *J. Phys. B* **31** 4489 (1998)
- [34] Japha Y, Choi S, Burnett K and Band Y B *Phys. Rev. Lett* **82** 1079 (1999)
- [35] Japha Y, Choi S and Burnett K *Phys. Rev. A* **61** 063606 (2000)
- [36] Robins N, Savage C and Ostrovskaya E A *Phys. Rev. A* **64** 043605 (2001)
- [37] S.A. Haine S A, Hope J J , Robins N P and Savage C M *Phys. Rev. Lett.* **88** 170403 (2002)
- [38] Graham R and Walls D F *Phys. Rev. A* **60** 1429 (1999)
- [39] Edwards M, Griggs D A, Holman P L, Clark C W, Rolston S L and Phillips W D *J. Phys. B* **32** 2935 (1999)
- [40] Nikolopoulos G M and Lambropoulos P *Phys. Rev. A* **61** 053812 (2000)
- [41] Nikolopoulos G M and Lambropoulos P *J. Opt. B: Quantum Semiclass. Opt* **115** 115 (2001)
- [42] Nikolopoulos G M and Lambropoulos P *J. Mod. Opt.* **49** 61 (2002)
- [43] Görlitz A, Vogels J M, Leanhardt A E, Raman C, Gustavson T L, Abo-Shaeer J R, Chikkatur A P, Gupta S, Inouye S, Rosenband T and Ketterle W *Phys. Rev. Lett* **87** 130402 (2001)
- [44] Schreck F, Khaykovich L, Corwin K L Ferrari G, Bourdel T, Cobizolles J and Salomon C *Phys. Rev. Lett* **87** 080403 (2001)
- [45] Ott H, Fortagh J, Schlotterbeck G, Grossmann A, and Zimmermann C *Phys. Rev. Lett.* **87** 230401 (2001)
- [46] Hänsel W, Hommelhoff P, Hänsch T W and Reichel J *Nature* **413** 501 (2001)
- [47] Schneider S, Kasper A, vom Hagen Ch, Bartenstein M, Engeser B, Schumm T, Bar-Joseph I, Folman R, Feenstra L and Schmiedmayer J *Phys. Rev. A* **67** 023612 (2003)
- [48] For early literature on the appearance of Bose-Einstein condensation in low-dimensional potentials, the reader is referred to: Ketterle W and van Druten N J *Phys. Rev. A* **54** 656 (1996); Ingold G-L and Lambrecht A *Eur. Phys. J. D* **1** 29 (1998)
- [49] Petrov D S, Shlyapnikov G V and Walraven J T M *Phys. Rev. Lett.* **85** 3745 (2000)
- [50] Al Khawaja U, Andersen J, Proukakis N P and Stoof H T C *Phys. Rev. A* **66** 013615 (2002)
- [51] Proukakis N P, *Laser Phys.* **13** 527 (2003); Proukakis N P and Stoof H T C (in preparation, 2003)
- [52] Band Y B, Julienne P S and Trippenbach M *Phys. Rev. A* **59** 3823 (1999)
- [53] Jeffers J, Horak P, Barnett S M and Randmore P M *Phys. Rev. A* **62** 043602 (2000)
- [54] Olshanii M *Phys. Rev. Lett.* **81** 938 (1998)
- [55] Proukakis N P, Burnett K and Stoof H T C *Phys. Rev. A* **57** 1230 (1998)
- [56] Morgan S A *J. Phys. B* **33** 3847 (2000)
- [57] Ruostekoski J, Gasenzer T and Hutchinson D A W (unpublished)

Figure captions

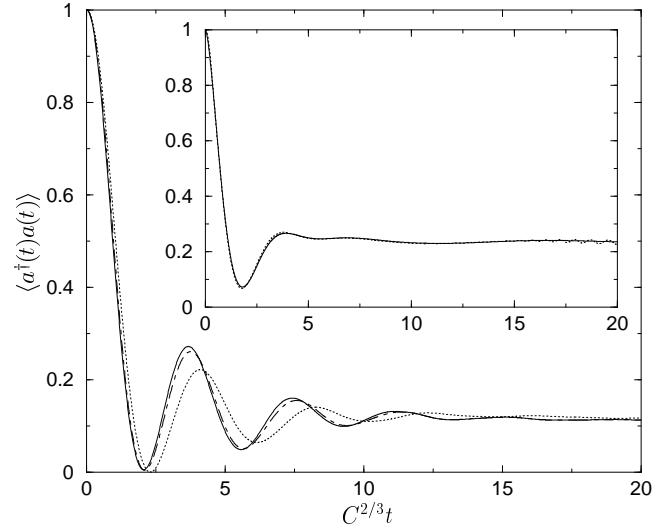


Figure 1. The normalized mean number of atoms in the condensate as a function of the dimensionless time $C^{2/3}t$ for Gaussian ($\Gamma = 10^6 \text{sec}^{-2}$) and broad-band (inset) couplings. The solid lines correspond to the exact solutions obtained by means of the Laplace transform. We also plot the discretization solutions for $N = 50$, $\omega_{low} = 0$ and $\omega_{up} = 3.0C^{2/3}$ (dotted line) as well as for $N = 1000$, $\omega_{low} = 0$ and $\omega_{up} = 3.0C^{2/3}$ (dot-dashed line), respectively. Inset: $N = 50$, $\omega_{low} = 0$ and $\omega_{up} = 10.0C^{2/3}$ (dotted line)

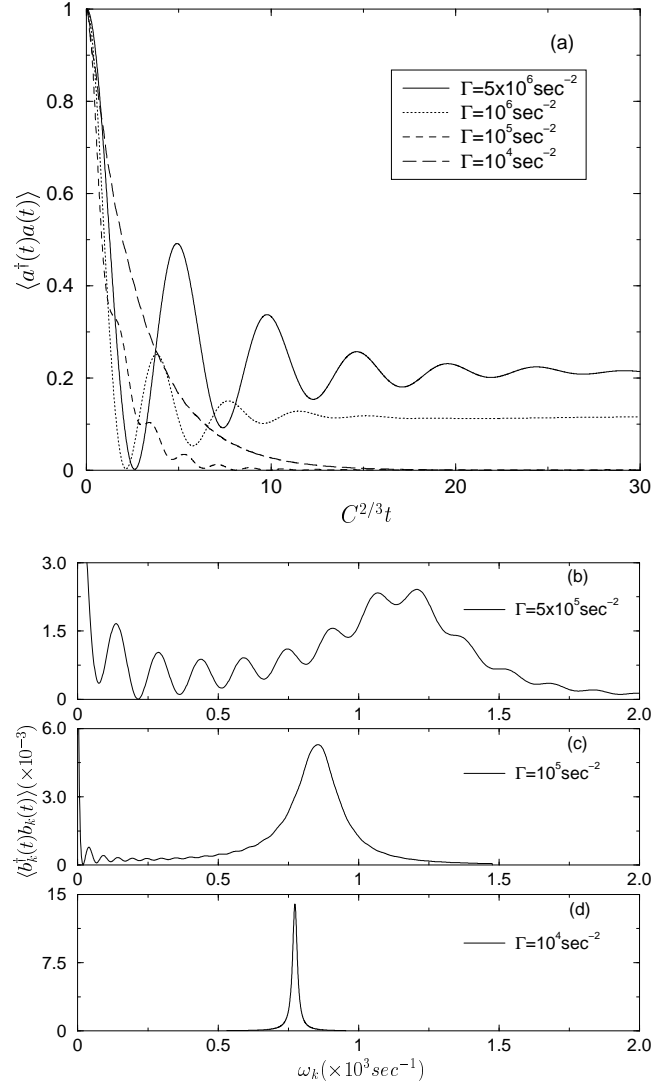


Figure 2. The evolution of the normalized trap population, as a function of the dimensionless time $C^{2/3}t$ (a) and the energy distribution of the outcoupled atoms at $t = 30C^{-2/3}$ [(b)-(d)], for Gaussian coupling and various coupling strengths. The calculations are for 1000 discrete modes, $\omega_{low} = 0$ and $\omega_{up} = 18C^{2/3}$ ($\Gamma = 10^4 \text{ sec}^{-2}$), $\omega_{up} = 6C^{2/3}$ ($\Gamma = 10^5 \text{ sec}^{-2}$), $\omega_{up} = 3C^{2/3}$ ($\Gamma = 5 \times 10^5 - 5 \times 10^6 \text{ sec}^{-2}$).

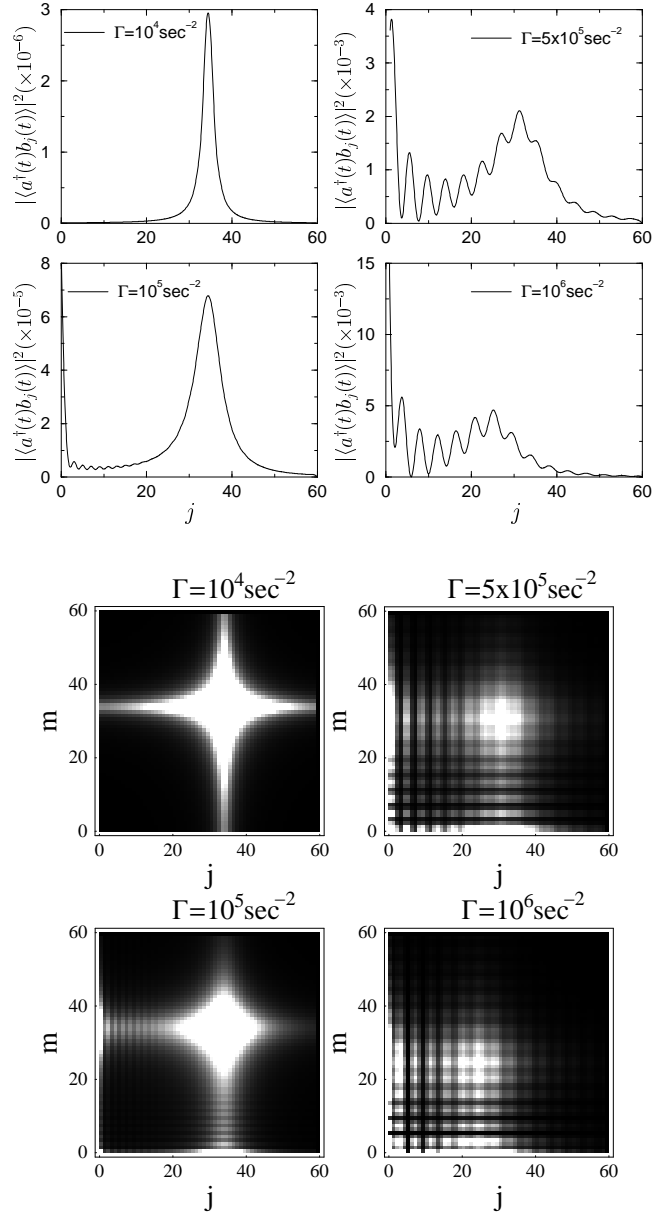


Figure 3. The magnitude of the matrix elements $\langle a^\dagger(t)b_j(t) \rangle$ (upper) and $\langle b_m^\dagger(t)b_j(t) \rangle$ (lower) for Gaussian coupling at $C^{2/3}t = 30$ and various coupling strengths Γ . For the lower graphs, dark and white regions represent matrix elements with negligible and large magnitude respectively. The calculations are for 60 discrete modes and cutoff frequencies: $\omega_{low} = 10C^{2/3}, \omega_{up} = 18C^{2/3}$ ($\Gamma = 10^4 sec^{-2}$); $\omega_{low} = 0, \omega_{up} = 6C^{2/3}$ ($\Gamma = 10^5 sec^{-2}$); $\omega_{low} = 0, \omega_{up} = 3C^{2/3}$ ($\Gamma = 5 \times 10^5 - 10^6 sec^{-2}$).

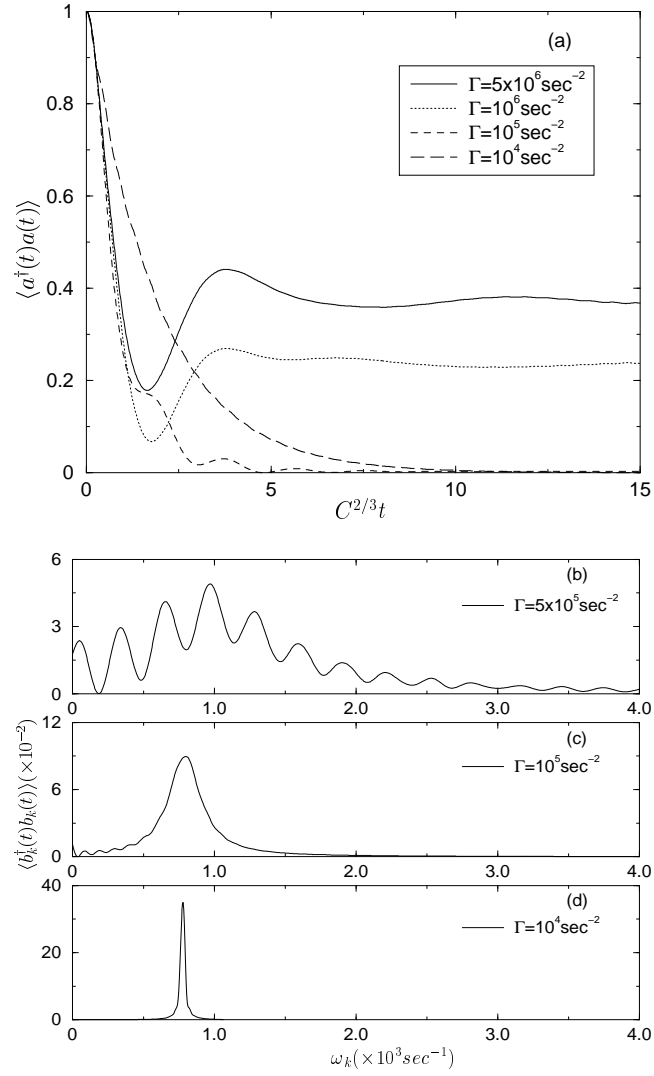


Figure 4. The evolution of the normalized trap population, as a function of the dimensionless time $C^{2/3}t$ (upper graph) and the energy distribution of the outcoupled atoms at $t = 15C^{-2/3}$ (lower graph), for broad-band coupling and various coupling strengths. The calculations are for 100 discrete modes, $\omega_{low} = 0$ and $\omega_{up} = 20C^{2/3}$.

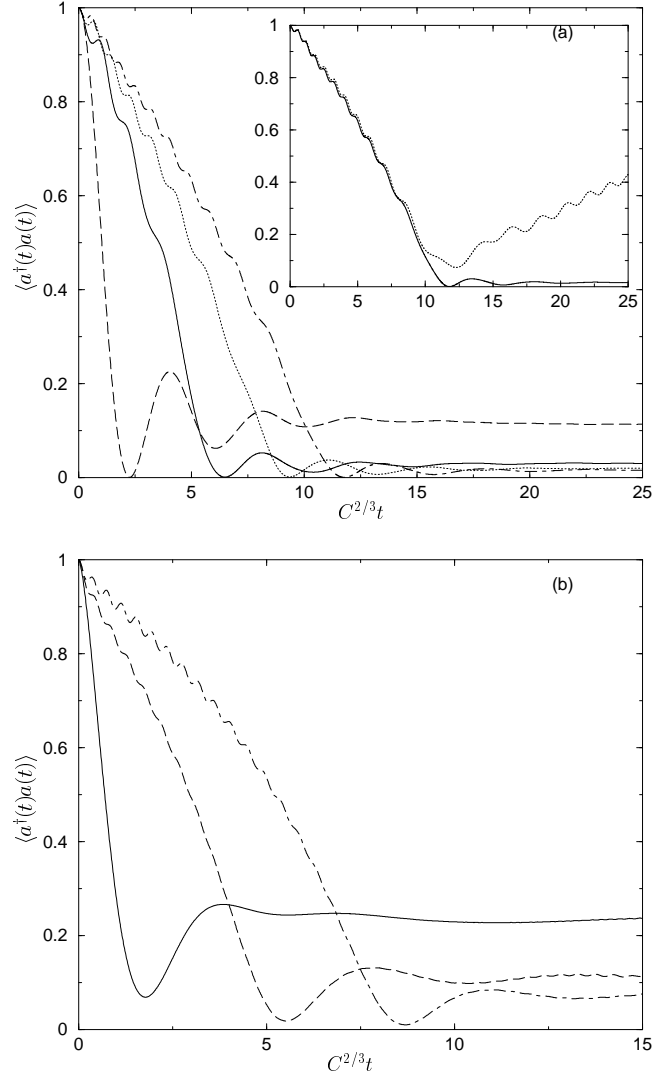


Figure 5. Effect of trap-free interatomic interactions on the time-evolution of the normalized trap population for Gaussian (a) and broad-band (b) couplings. All calculations have been obtained in the context of set B. (a) The coupling constant is $\Gamma = 10^6 \text{ sec}^{-2}$ and the population is plotted for various interatomic-coupling strengths: $C_M = 0$ (long-dashed line), $C_M = 4C^{2/3}$ (solid line), $C_M = 8C^{2/3}$ (dotted line) and $C_M = 12C^{2/3}$ (dot-dashed line). Discretization parameters: $N = 60$, $\omega_{low} = 0$, $\omega_{up} = 3C^{2/3}$. Inset: The solid and the dotted lines correspond to a propagation of set B and equations (48)-(50) respectively, for $\Gamma = 10^6 \text{ sec}^{-2}$ and $C_M = 12C^{2/3}$. (b) The solid line is for $C_M = 0$, the dashed line for $C_M = 1C^{2/3}$ and the dot-dashed line for $C_M = 2C^{2/3}$. Discretization parameters: $N = 60$, $\omega_{low} = 0$, $\delta\omega = 0.004C^{2/3}$.

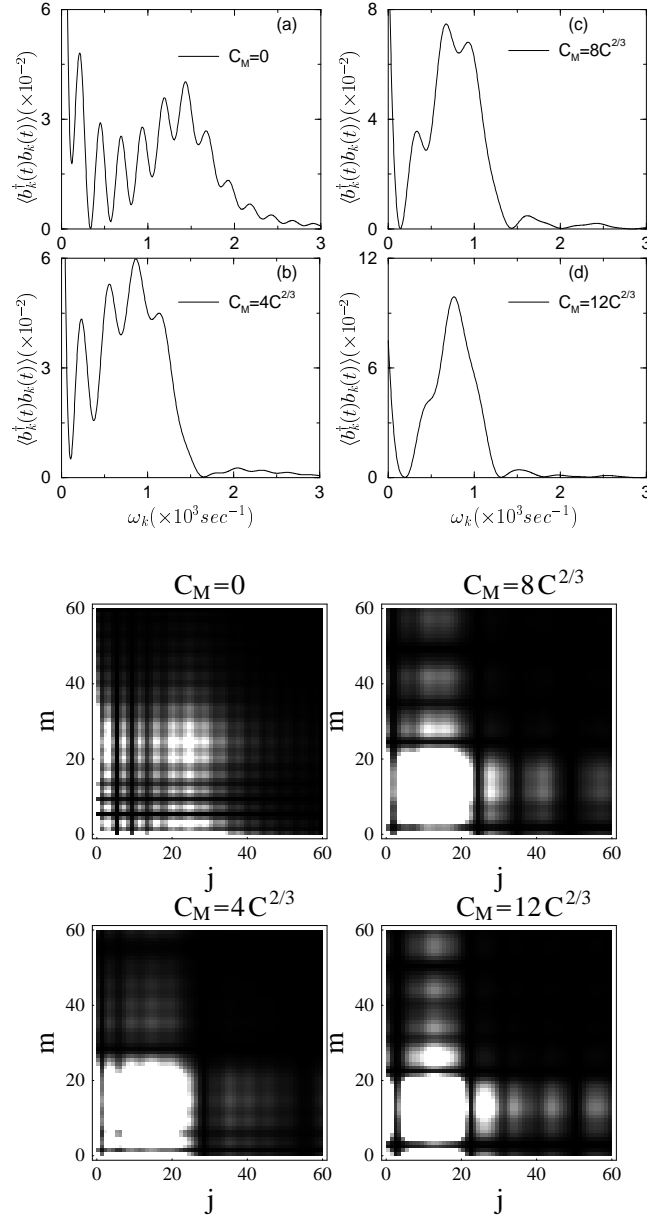


Figure 6. Effect of trap-free interatomic interactions on the energy distribution of the outcoupled atoms (upper graphs) and the magnitude of the matrix elements $\langle b_m^\dagger(t)b_j(t) \rangle$ (lower graphs). All the graphs are for Gaussian coupling ($\Gamma = 10^6 \text{ sec}^{-2}$) and correspond to $C^{2/3}t = 25$ and various interatomic-coupling strengths. Dark and white regions in the lower graphs represent matrix elements with negligible and large magnitude respectively. Discretization parameters as in figure 5.